Drag Reduction by Injection

Steven Deutsch, Arnold A. Fontaine, Michael J. Moeny and Howard L. Petrie
The Applied Research Laboratory,
The Pennsylvania State University,
University Park, PA 16804

Drag reduction experiments, using the combined injection of long chained polymers and gas to form microbubbles, on a 3.1m large flat plate in the 48" diameter water tunnel at the Applied Research Laboratory of the Pennsylvania State University are described. Gas injection upstream of polymer injection produces increased levels of drag reduction which can be higher than that expected for independent processes; that is, synergy. Synergy is a result of the gas layer induced extension of the polymer alone initial diffusion zone in combination with the increased drag reduction by microbubbles.

INTRODUCTION

The introduction of solutions of long-chained polymer molecules or of gas to form microbubbles into a turbulent boundary layer has been long known to reduce skin-friction drag. The mechanisms responsible for drag reduction by either of these methods are not yet fully understood. However, Tiederman et al. (1985) and Smith and Tiederman (1990) showed that polymer molecules are effective only when located in the buffer region of the turbulent boundary layer and Pal et al. (1989) reached essentially the same conclusion regarding microbubbles.

The first detailed studies of slot injected polymer drag reduction were those of Wu and Tulin (1972), who considered drag reduction as a function of polymer concentration and injection flow rate. Poreh and Hsu (1972) considered the diffusion aspects of the polymer injection problem. Their work was modeled after the classical experimental results of Poreh and Cermak (1964) for the diffusion of a passive contaminant from a line source. Poreh and Cermak (1964) characterized the process by identifying, as a function of diffusion layer thickness to boundary layer thickness, four diffusion zones. For the initial diffusion zone, the contaminant resides in a thin layer at the wall on the order of the viscous sublayer. Poreh and Hsu determined that the diffusion zone results of Poreh and Cermak were qualitatively useful in characterizing the polymer diffusion process. Whereas for a passive contaminant the initial

diffusion zone is on the order of millimeters, Poreh and Hsu estimated that the initial diffusion zone for polymer could be up to 3 orders of magnitude larger.

Fontaine, Petrie and Brungart (1992) used laser Doppler velocimetry to analyze the slot injected case in an external boundary layer. They showed that the primary effect of injected polymer is the suppression of vertical velocity fluctuations and of corresponding Reynolds stress in the near wall region. Turbulent transport properties are also suppressed, which results in a reduction in the diffusion of the polymer away from the wall. This result is quite significant as Vdovin and Smol'yakov (1977, 1981) and Petrie et al. (1996) have identified the initial diffusion zone as the region of high drag reduction. We reproduce the results of Petrie et al. as Figure 1. Here, concentration has been measured by doping the polymer with fluorescent dye and using an optical technique described by Brungart et al. (1991).

The initial zone in both drag reduction and near wall concentration is apparent through a K of about 10, after which both the drag reduction and the near wall polymer concentration drop of rapidly. This rapid change in the slope of the drag reduction versus K curve, at K=10, denotes a change from initial zone to transition zone behavior in the diffusion process, Poreh and Hsu (1972) and Vdovin and Smol'yakov (1981). Our experience with polyethylene oxide (PEO) is that the more effective polymers at reducing drag (higher molecular weight) are more effective solely through having longer initial zones (K < 10), as seen in the shift in K from ~10 to ~ 5 for the comparison of PEO WSR 301 with PEO WSR 309 in Figure 2. The parameter $K=QC_i/\rho U_e X$ (or $QCi/\mu\ (1/Re_x)$), used in Figure 1, was first developed by Vdovin and Smol'yakov (1978, 1981). Here Q is the polymer flow rate per unit span of the injection slot, C_i the injection concentration in units of density, U the mean velocity and X_s the distance from the slot. Here, the numerator represents the consumption rate, while the denominator is related to the diffusion process.

High levels of microbubble drag reduction have been achieved by the direct injection of gas through slots or porous materials (Merkle and Deutsch, 1989; Migirenko and Evseev 1974; Bogdevich et al. 1976 a,b). The primary parameter is the actual gas flow rate (Qa) referenced to the ambient conditions of temperature and pressure at the injector (Madavan et al. 1985a; Fontaine and Deutsch, 1992). Microbubble drag reduction does not appear to be strongly influenced by gas type (Fontaine and Deutsch 1992) or method of injection (Merkle and Deutsch, 1989). Observed bubble dimensions range from fifty to several hundred wall units in size. Clark and Deutsch (1991) showed that microbubble drag reduction exhibits a strong sensitivity to applied axial pressure gradient. Pal et al. (1989) found that the frequency spectra and higher order moments of the wall shear stress fluctuation statistics in microbubble

drag reduction were remarkably similar to that observed with polymer injection. Merkle and Deutsch (1989) provide a comprehensive review of early attempts at skin friction reduction by microbubble injection.

Recently, Petrie et al. (2003) investigated heterogeneous polymer drag reduction over surface roughness. One smooth and three rough surfaces were tested ranging from transitionally rough through fully rough. They report that the drag force for all surfaces approaches the same value with increasing K-factor, so that the percentage drag reduction is greater for the rough surfaces than for the smooth. A follow-on study by Deutsch et al. (2004) investigated the effects of microbubble injection over rough surfaces using the same facility and surfaces as in Petrie et al. (2003). To help compare with the polymer data, Deutsch et al. (2004) introduce a microbubble K factor as Q/bUX. They reported similar results to the polymer study, in that for a given velocity the measured drag force asymptotes to nearly the same value for all surfaces with increasing gas flow rate. The details of the initial zone behavior for each, however, is quite different in that the polymer showed a decreasing extent of initial zone for increasing roughness, while the bubble initial zone was uninfluenced.

Fontaine et al. al. (1999) reported the effect of microbubble injection into a homogeneous polymer "ocean" on an axisymetric body. The authors found measured drag reduction levels for combined injection were higher than levels for either polymer or microbubbles alone. The increase in drag reduction was found to follow a multiplicative relationship (equation 1.1) with no evidence of synergy or cooperative action.

$$\left(\frac{Cf}{Cfo}\right)_{absolute} = \left(\frac{Cf}{Cfo}\right)_{polymer\ alone} * \left(\frac{Cf}{Cfo}\right)_{microbubble\ alone} \qquad 1.1$$

These results suggest that the drag reduction with homogeneous polymer ocean acts independently of the mechanism induced by microbubble injection. Quite similar results are obtained for polymer injected into a homogeneous polymer solution (Petrie et al. (2003)).

Philips et al. (1998) measured drag reduction with combined microbubble and polymer injection in sea-water on a 2.73m long flat plate. PEO WSR 301 at 1000 wppm was injected with air injection either upstream or downstream of the polymer injection. When configured for gas injection upstream of polymer injection, they reported the consistent observation of synergy and found the presence of synergy to be effectively confined to levels of microbubble injection which produced less than 30% drag reduction. They noted that the highest levels of synergy were achieved for low microbubble injection rates over nearly all polymer injection rates. Synergy was defined as the reduction in drag during combined injection greater than the sum of the drag reduction observed during individual injection, or an

additive interaction. Air injection downstream of the polymer injection produced lower levels of drag reduction than the sum of the individual reductions.

In the following study, we use the term synergy for a combination of injectants that produce a level of drag reduction greater than the product of the effect of each material injected separately:

$$synergy = \left(C_f / C_{f\ og} * C_f / C_{f\ op} \right) - C_f / C_{f\ ogp} \quad . \qquad 1.2$$

Since Fontaine et al. al. (1999) has shown that the drag reduction due to the injection of microbubbles into a polymer ocean is multiplicative, this definition is self-consistent. The influence of combined injection on the persistence of the drag reduction is examined. To best study persistence, we chose to use the inverse of the K factor as our independent parameter. This removes a singularity at the injector and seems to us more intuitive. Vdovin and Smol'yakov (1977, 1981) also considered this by introducing a diffusion length L, as $L=QC_i/\rho U_e$, and plotting their drag reduction data as Xs/L.

EXPERIMENTAL APPROACH

Experiments were conducted with a large flat plate installed in the 48" diameter water tunnel at ARL Penn State. The test section has a diameter of 1.22m (48") and a length of 4.27m. The 0.07m thick plate is 3.1m long by 1.22m span and is mounted on the horizontal center plane of the tunnel with the working surface up, opposite gravity. The leading edge consists of an elliptical nose section. A near zero pressure gradient is maintained along the plate using an adjustable, wedge-shaped tail section at the trailing edge. Flow over the central 50% of the plate is turbulent, two-dimensional and fully developed as characterized by a series of laser Doppler velocimetry surveys described in Petrie et al. (1996). Momentum thickness Reynolds numbers are as high as 39,000.

Polymer and microbubble injection is accomplished through a dual-injector assembly located roughly 0.6 m from the plate leading edge. The upstream slot is ~0.6 m from the leading edge of the plate, while the second slot is 39 mm further downstream. This separation is approximately four boundary-layer thicknesses at 10.7 m/s. The slot design is described in Petrie et al. (2003). Visual inspection of the bubble cloud and of an injected polymer and dye solution served to verify span wise uniformity. Skin friction is measured by six identical floating element drag balances installed in three modules flush-mounted with the upper surface of the flat plate. The distances from the plate leading edge to the leading edge of each

balance were: X_{LE} = 0.7, 0.87, 1.09, 1.466, 1.71, 2.50 m. Each drag balance consists of a 127mm wide by 38mm long floating element mounted to a strain gauged shear flexure which is in turn rigidly mounted to the drag balance module assembly installed in the flat plate. The sides of the floating elements are beveled slightly to produce a knife-edge at the upper surface. Drag balances were calibrated with weights prior to installation and were linear to an R^2 >0.999. During installation of the drag balances, a gap of between 0.05 to 0.125mm was maintained around the shear plates. Each shear plate was flush with the surrounding surface.

Solutions of PEO WSR 309, with a mean molecular weight of about eight million, were hand-mixed in 100 liter vats, as described by Petrie et al. (2003). Chlorine is known to negatively affect polyethylene oxide solutions, Petrie (2003). The water was dechlorinated with sodium thiosulfate. The mix was then allowed to stand for several hours to hydrate. To avoid degradation of the solution, a peristaltic pump was used to transfer the polymer from the mixing vat to the injection tank. This procedure has proven to produce consistent results.

Data were taken at free-stream velocities of 10.7, 13.7 and 16.2 m/s for a Reynolds number range of approximately 6.6 to 33.4 million, based on stream wise distance from the turbulent boundary layer virtual origin (64 mm upstream of plate leading edge) to the leading edge of the force cells. Air injection volumetric flow rates were roughly Qa = 0.0035, 0.0073 and 0.013 m^3/s, corrected to tunnel conditions. Note that each successive injection rate is roughly twice the preceding rate. The three air flow rates are referred to as Low, Medium and High respectively in the figures. Polymer injection rates were 5 and 10 Qs, where Qs is the volume flow rate through the viscous sublayer defined as $0< y^+ \leq 11.6$. Qs may be simply shown to be independent of velocity. To avoid cavitation at the higher velocities, tunnel static pressure was maintained at 35 psi as measured at the leading edge of the plate.

RESULTS AND DISCUSSSION

Typical single injection drag reduction results taken at a free stream velocity of 16 m/s are shown in Figures 3a&b for polymer and for microbubble injection. These figures illustrate the similarities and differences between the drag reduction techniques with distance from the slot. Repeatability of the injection tests is indicated by the error bars to 95% confidence levels. Figure 3a shows drag reduction as a function of stream wise distance for polymer injection of 500, 1000 and 2000 wppm PEO WSR 309 at 5 and 10 Qs. Figure 3a exhibits a downstream displaced peak in the drag reduction curves for 1000 and 2000 wppm, while the 500 wppm data peaks at the first measurement location. We suspect that the lower levels of drag reduction close to the slot for the higher concentration cases are a result of

increased near wall viscosity ($\tau_w = \mu(dU/dy)$. Note that substantial drag reduction is still observed at the furthest locations for the higher polymer consumption rates (QC_i).

In contrast, local drag reduction levels from microbubble injection are highest at the upstream most balance and decrease steadily with increasing Xs, as shown in Figure 3b. In addition, drag reduction by microbubble injection near the slot increases with increasing injection rate, whereas increased polymer concentration can decrease the drag reduction near the slot. We note that the drag reduction is nearly zero, independent of gas flow rate, at the position of the last balance.

Combined Injection

We plot the drag reduction data against Xs/L in Figures 4 & 5. Here we use Lp for polymer and Lm for microbubbles. In lieu of normalization for combined injection, it is useful to examine the combined injection drag reduction plotted against each of these variables.

Figure 4 presents single and combined injection data in terms of drag reduction vs. Xs/Lp. Solid symbols represent combined injection: lines indicate polymer injection. The plotted data cover a range of U from 10.7 to 16m/s, Q of 5 & 10 Qs and X up to 1.9m. The striking feature of this plot is that combined injection drag reduction does not generally decrease below Xs/Lp < 0.1 as it does for polymer injection alone. The body of the combined injection data cloud is also elevated relative to the polymer-only lines, indicating a higher level of drag reduction is achieved for a given Xs/Lp. The lowest Xs/Lp are representative of data taken at low speeds or close to the injector. The decreased drag reduction in the polymer-only lines for Xs/Lp < 0.1 is an indicator of high viscosity for the high polymer concentration data. The data shows that combined injection effectively eliminates the low Xs/Lp drag reduction penalty. The shift to higher Xs/Lp at the start of the transition zone, $0.3 \leq Xs/LP \leq 0.5$, indicates an extension of the initial diffusion zone with combined injection. Thus, addition of gas at constant U and polymer injection rate increases the length of the initial diffusion zone.

Figure 5 presents the gas and combined injection data against Xs/Lm. The symbols are combined injection data, the lines are gas injection alone. This plot shows that the drag reduction levels for the combined injection approximately match those of the most effective regime of microbubble injection, low Xs/Lm < 200, which is close to the injection slot. The most dramatic feature, however, is the much slower decrease in drag reduction with increasing Xs/Lm when compared with microbubble injection alone.

Figure 6 plots synergy, defined earlier as the difference between the multiplicative and measured skin friction reductions, against Xs/Lp for 500 wppm polymer and all gas flow rates. The Low gas flow rate case produces the lowest levels of synergy, generally less than 10%. This Low gas injection is also the only case which does not exhibit negative levels of synergy at the upstream most balance. Recall that negative synergy simply means that the multiplicative drag reduction value is greater than the measured value. The Medium and High gas injection rates produce the highest levels of synergy, peaking at 25-30%. The synergy lines in the combined 10Qs polymer with Medium and High gas flow rates peak at nearly a factor of 2 increase in Xs/Lp when compared to the Low injection case. This shift to higher Xs/Lp suggests a reduction in the polymer diffusion away from the wall or a lengthening of the initial diffusion zone to further downstream. The corresponding negative synergy levels at Xs/Lp < 0.1 indicate that the benefit of reduced diffusion by gas injection may not occur in the initial diffusion zone, and the increased polymer viscosity may act to offset drag reduction benefits obtained by the gas injection.

Figure 7 presents combined injection data for 1000 wppm polymer in the same manner. Note that all cases exhibit some degree of negative synergy close to the slot. The trend in increasing synergy with increasing gas injection rate from L to M and H is observed.

Figure 8 presents combined injection data for 2000 wppm polymer. It is clear from this plot that the end of the initial zone has been pushed past the end of the plate. The synergy traces for nearly all conditions, with the possible exception of the L/5Qs at 16 m/s, show no signs of peaking. Interestingly, the synergy levels are roughly zero near the slot for all conditions. This indicates that the multiplicative condition is being realized at that location.

Examination of the data in Figures 6-8 illustrate that the ability to produce synergy is dependent on the initial state of the polymer injected initial diffusion zone before gas injection. The 500 wppm data indicate that combined injection yields increased drag reduction levels that follow roughly a multiplicative behavior, very small positive or negative synergy, in the initial diffusion zone. As the end of the polymer only initial diffusion zone is approached, the addition of gas effectively reduces the polymer diffusion and moves the end of the initial diffusion zone further downstream, producing increased drag reduction levels above the multiplicative level. The data suggests that synergy is maintained through the transition zone as well. Interestingly, synergy does not start until Xs/Lp ~ 0.15 to 0.2 ($5 \leq Kp \leq \sim 7$), which is in the end of the polymer injection initial diffusion zone (see Figure 2). It peaks at Xs/Lp ~ 0.4 (Kp ~ 2.5), which is the end of the combined injection initial diffusion zone (see Figure 7).

We reason that in the polymer injection initial diffusion zone downstream of the slot, addition of gas produces a multiplicative result only because the polymer alone has reached a state of maximum drag reduction. Therefore, decreased diffusion or increased near wall concentration cannot produce an additional level of polymer based drag reduction. Thus, injection of gas increases the overall drag reduction by the independent multiplicative effect near the slot. This multiplicative result is similar to that observed in the homogeneous polymer drag reduction / gas injection results of Fontaine and Deutsch (1999). The slight negative synergy observed is most likely a viscous effect due to the increased concentration of high viscosity polymer at the wall.

Increases in the near wall concentration of the polymer, at locations downstream of the polymer only initial diffusion zone, will result in increased polymer based drag reduction, since the polymer is not at maximum drag reduction. Therefore at the end of the polymer only initial diffusion zone and throughout the transition zone, addition of gas decreases polymer diffusion and produces an increase in drag reduction that can be attributed to two sources: the independent addition of the microbubble based drag reduction (which is falling off rapidly); and the increase due to the increased polymer based drag reduction as a result of the increased wall concentration. It is this dual contribution to the increased drag reduction that produces the synergistic effect.

The increase in drag reduction persistence under combined injection is one of its most useful characteristics. The increased persistence can be assessed by comparing the value of Xs/Lp or Xs/Lm that provide the same total drag reduction along the plate for polymer, gas and combined injection. A least squares polynomial curve is fit to the measured local drag reduction as a function of either Xs/Lp (polymer and combined) or Xs/Lm (gas). The total drag reduction is then calculated by integrating this curve fit from 0 to a selected Xs/Lp or Xs/Lm, $DR_{total} = X_s / L_p \int_0^{Xs/Lp} DR \;\; d\left(X_s / l_p\right)$ for polymer or combined injection and $DR_{total} = X_s / L_m \int_0^{Xs/Lm} DR \;\; d\left(X_s / l_m\right)$ for gas injection. An estimate of the increased persistence for a defined drag level can then be obtained by computing the above integrals from 0 to the value of Xs/Lp or Xs/Lm that yields the desired total drag reduction. An increase in Xs/Lp with combined injection for the desired drag reduction level translates into the same increase in X (or persistence) for constant polymer QCi, gas injection and free stream speed.

A comparison of Xs/Lp and Xs/Lm corresponding to an integrated drag reduction of 48% is provided in Table 1 for characteristic gas, polymer and combined injection cases. The Xs/Lp and Xs/Lm columns also contain the estimated stream wise position (Xs) calculated from those Xs/Lp and Xs/Lm values using the defined velocity and injection parameters in Table 1. The results indicate that significant increases in persistence can be obtained by combining the two systems, or conversely, higher levels of total drag reduction can be obtained for a specified axial length. For example, the distance from the slot, Xs, at which 48% integrated drag reduction is observed with 500 PEO WSR 309 injection alone is 0.227m. Combining this polymer injection with a gas injection at the Medium rate increases this distance to Xs= 2.2m. In addition, higher total drag reduction can be obtained with lower polymer QCi for the combined system then what is achieved with higher polymer QCi values for polymer injection alone. This increased effectiveness implies that by combining gas injection upstream of a polymer drag reduction system, the total system requirements can be reduced, less polymer needs to be carried and delivered with reduced polymer pumping losses.

Table 1: Comparison of 48%Total Drag Reduction for Polymer, Gas and combined Injection

Polymer Conc	Polymer Qs	Gas flow Rate	Ue	Polymer		Gas		Combined	
				Xs/Lp	Xs(m)	Xs/Lm	Xs(m)	Xs/Lp	Xs(m)
500	10	M	16	0.1	0.227	620	0.527	0.97	2.2
1000	5	M	16	0.27	0.628	620	0.527	1.0	2.33
2000	5	M	16	0.27	1.16	620	0.527	0.77	3.3

CONCLUSIONS

Injection of gas upstream of polymer injection produces increased levels of drag reduction with increased persistence. Under the right conditions, the increased level of drag reduction can be significantly higher than the multiplicative result expected for combined independent processes. The increased level of drag reduction and persistence is more than can be achieved by microbubble or polymer alone and implies that significant levels of total drag reduction can be obtained at more moderate expenditure rates of both polymer and microbubbles when combined. A system can be implemented at lower overall cost by reducing material delivery

cost through lower polymer concentration (lower viscosity), lower polymer injection rate, and reduced gas requirements. In addition, the combination of gas with polymer injection eliminates the increased drag penalty associated with high concentration, high viscosity polymer solutions near the injector. These results suggest that the addition of microbubble injection upstream of polymer injection may reduce the rate of diffusion of the polymer away from the wall. This will shift the polymer only initial diffusion zone downstream and effectively increase near wall polymer concentration and larger drag reduction to longer distances from the injection slot.

REFERENCES

Bogdevich, V. G. and Evseev, A. R. (1976), "Effect of Gas Saturation on Wall Turbulence," Investigations of Boundary Layer Control, Thermophysics Institute, Novosibirsk (in Russian).

Bogdevich, V. G. and Malyuga, A. G. (1976), "The Distribution of Skin Friction in a Turbulent Boundary Layer," Investigations of Boundary Layer Control, Thermophysics Institute, Novosibirsk (in Russian).

Brungart, T., Harbison, W., Petrie, H., Merkle, C. (1991), "A Fluorescence Technique for Measurement of Slot-injected Fluid Concentration Profiles in a Turbulent Boundary Layer," Experiments in Fluids, 11: 9-16.

Clark, H. and Deutsch, S. (1991), "Microbubble Skin Friction Reduction on an Axisymmetric Body under the Influence of Applied Pressure Gradients," Physics of Fluids, A3(12), 2948-2954.

Deutsch, S., Money, M., Fontaine, A., Petrie, H. (2004), "Microbubble Drag Reduction in Rough Walled Turbulent Boundary Layers with Comparison against Polymer Drag Reduction," Experiments in Fluids, 37, 731-744.

Fontaine, A. A., Petrie, H. L., and Brungart, T. A. (1992), "Velocity Profile Statistics in a Turbulent Boundary Layer with Slot Injected Polymer," J. of Fluid Mechanics, 238, 435-466.

Fontaine, A., Deutsch, S., Brungart, T., Petrie, H., Fenstermacker, M. (1999), "Drag Reduction by Coupled Systems: Microbubble Injection with Homogeneous Polymer and Surfactant Solutions," Experiments in Fluids, **26**: 397-403.

Madavan, N. K., Deutsch, S. and Merkle, C. L. (1985), "Measurements of Local Skin Friction in a Microbubble Modified Turbulent Boundary Layer," J. of Fluid Mechanics, 156, 237-256.

Malyuga, A., Mikuta, V., Nenashev, A. (1989), "Local Drag Reduction at Flow of Polymer Solutions Aerated by Air Bubbles," 6th National Congress of Theoretical and Applied Mathematics, 25-30 September 1989, Varna, Bulgaria.

Merkle, C. L. and Deutsch, S. (1989), "Microbubble Drag Reduction," Frontiers in Experimental Fluid Mechanics, ed. M. Gad el Hak, No. 46, Springer Verlag, 291-335.

Migirenko, G. S. and Evseev, A. R. (1974), "Turbulent Boundary Layer with Gas Saturation," Problems of Thermophysics and Pjysical Hydrodynamics, Novosibirsk,
Nauka (in Russian).

Pal, S., Deutsch, S., Merkle, C. (1989), "A Comparison of Shear Stress Fluctuation Statistics Between Microbubble Modified and Polymer-Modified Turbulent Boundary Layers," Physics of Fluids A **1**(8).

Petrie, H., Fontaine, A. A., Brungart, T. (1996), "Drag reduction on a flat plate at high Reynolds number, with slot-injected polymer solutions," Proceedings of the ASME fluids engineering division summer meeting, ASME FED, Vol. 237, San Diego, California, July 1996, 2:3-9.

Petrie, H., Deutsch, S., Fontaine, A., Brungart, T. (2003), "Polymer Drag Reduction with Surface Roughness in Flat-Plate Turbulent Boundary Layer Flow," Experiments in Fluids, **35:** 8-23.

Philips, R., Castano, J., Stace, J. (1998), "Combined Polymer and Microbubble Drag Reduction," Proceedings of the International Symposium on Seawater Drag Reduction, 22-23 July 1998, Newport R.I.

Poreh, M. and Cermak, J. E. (1964), "Study of Diffusion from a Line Source in a Turbulent Boundary Layer," Intl. J. Heat Mass Transfer, 7, 1083-1095.

Poreh, M. and Hsu, K. (1972), "Diffusion of Drag Reducing Polymer into a Turbulent Boundary Layer," J. Hydronautics, 6, N1, 27-33.

Smith, R. and Tiederman, W. (1990), "Investigation into the mechanism of polymer thread drag reduction," Report PME-FM-90-1, Purdue University, School of Mechanical Engineering, West Lafayette, IN.

Sommer, S. and Petrie, H. (1992), "Diffusion of slot injected drag-reducing polymer solution in a LEBU modified turbulent boundary layer," Experiments in Fluids, **12**: 181-188.

Tiederman, W. G., Luchik, T. S., and Bogart, D. G. (1985), "Wall Layer Structure and Drag Reduction," J. of Fluid Mechanics, 156, 4-19-437.

Wu, J. and Tulin, M. P. (1972), "Drag Reduction by Ejecting Additive Solutions into Pure Water Boundary Layer," ASME Trans. J. of Basic Engineering, 749-756.

Vdovin, A. and Smol'yakov, A. (1978), "Diffusion of polymer solutions in a turbulent boundary layer," Zh. Prikl. Mekh. Tekh. Fiz. **2**, 66-73 (transl. in UDC 532.526, pp. 196-201, Plenum).

Vdovin, A. and Smol'yakov, A. (1981), "Turbulent diffusion of polymers in a turbulent boundary layer," Zh. Prikl. Mekh. Tekh. Fiz. **4**, 98-104 (transl. in UDC 532.526 (1982), pp. 526-531, Plenum).

White (1974), Viscous Fluid Flow, McGraw-Hill, Inc.

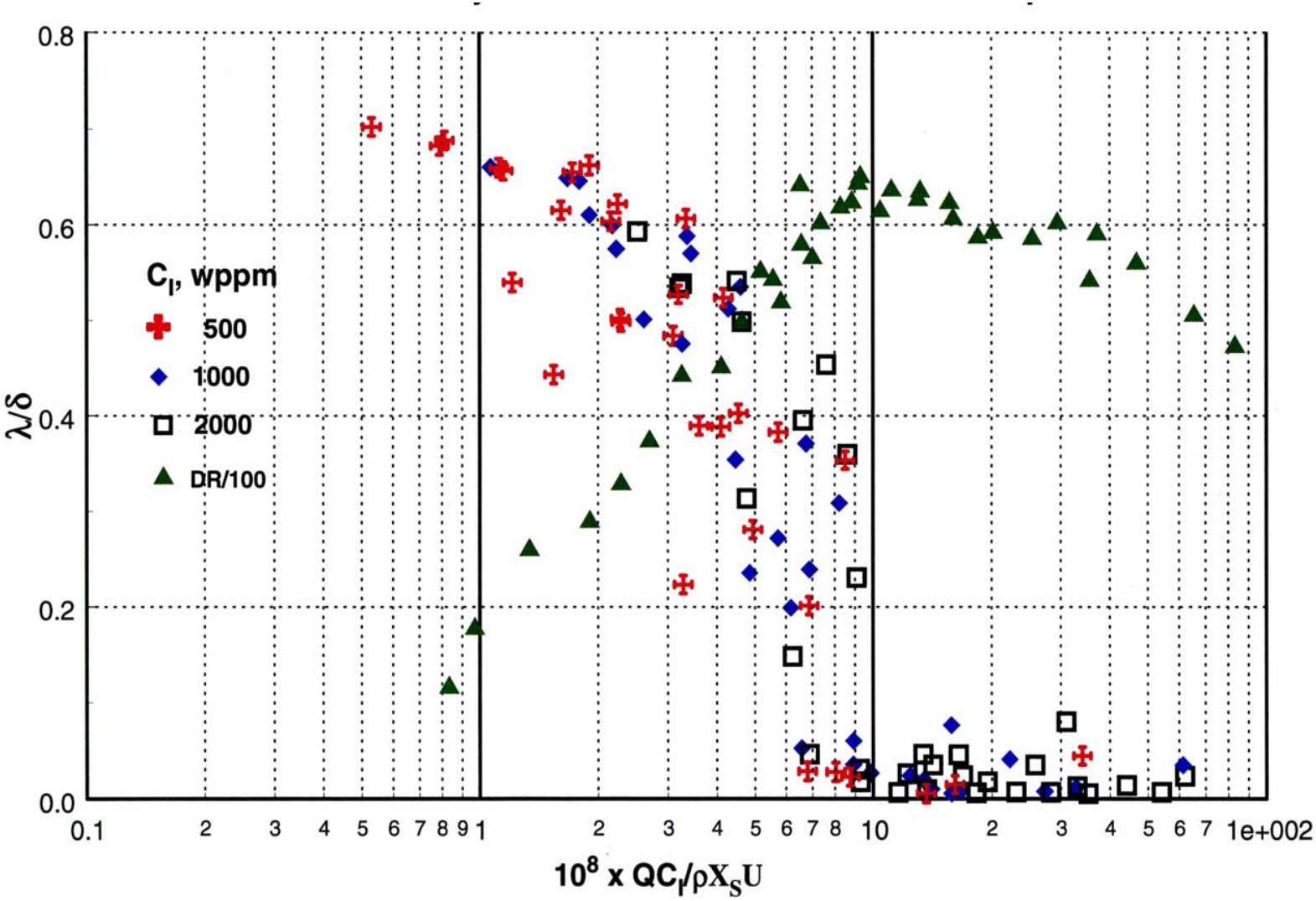

Figure 1. Diffusion layer development versus K factor compared to local drag reduction with PEO WSR 301 injection Petrie et al. (1996).

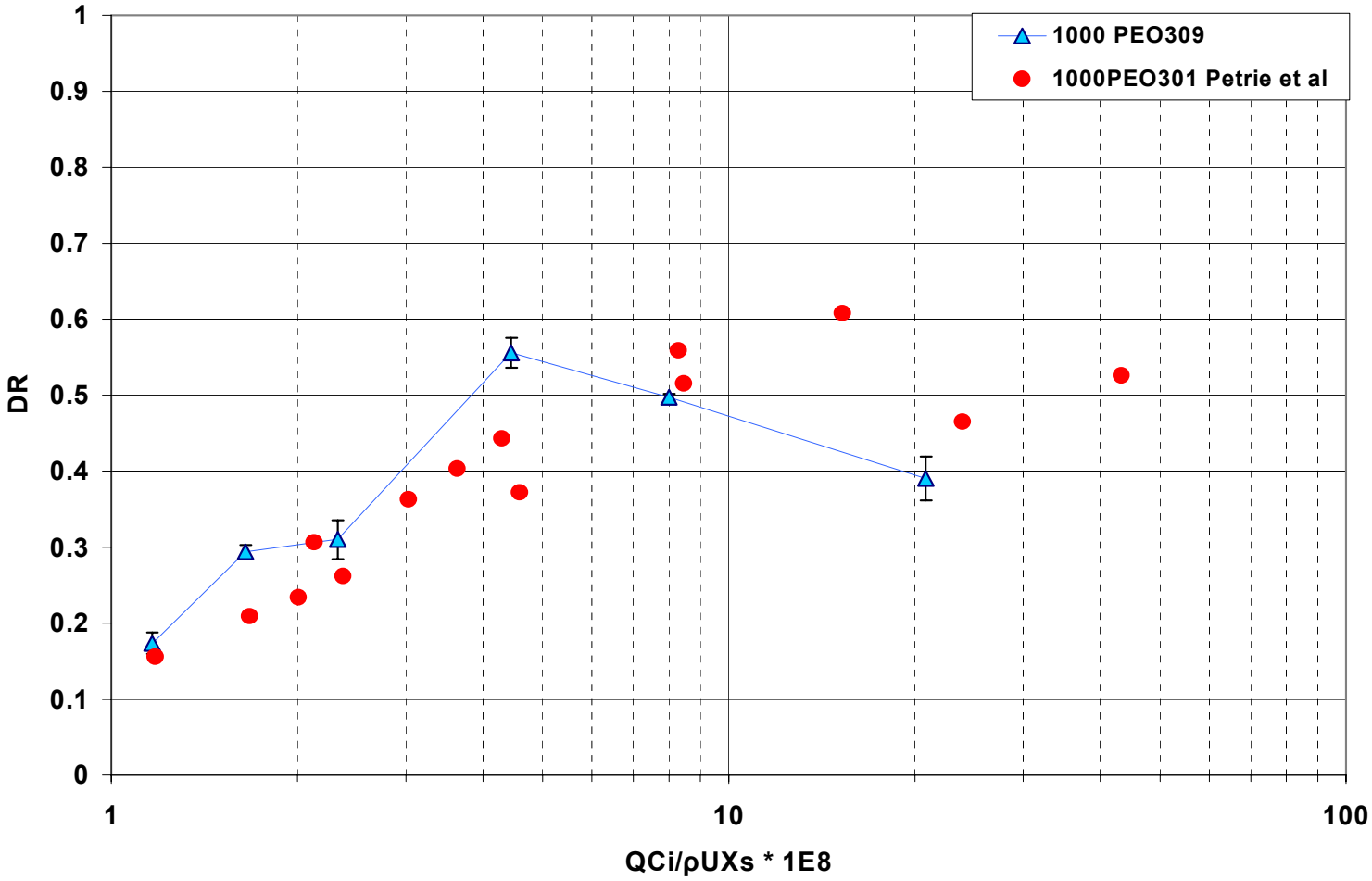

Figure 2. Comparison of drag reduction versus K factor for PEO WSR 301 and PEO WSR 309.

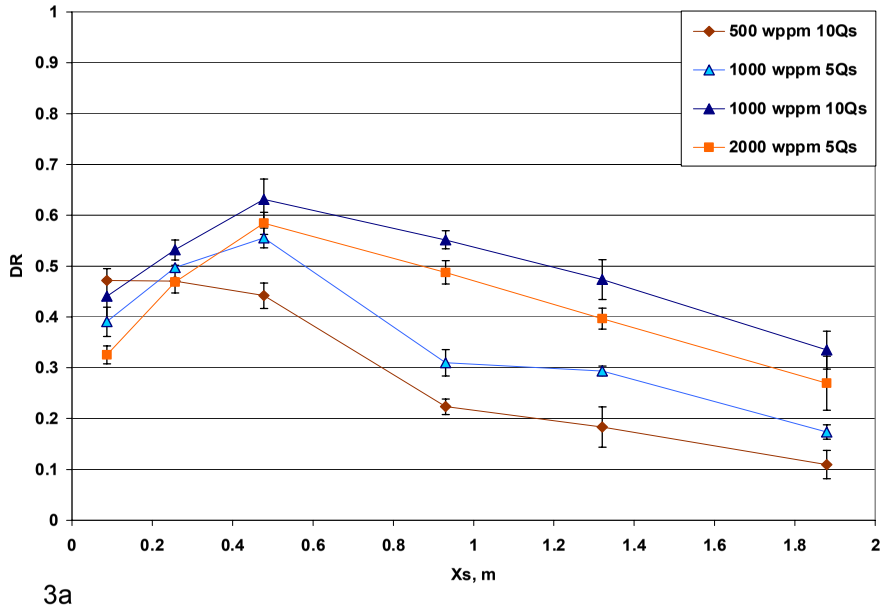

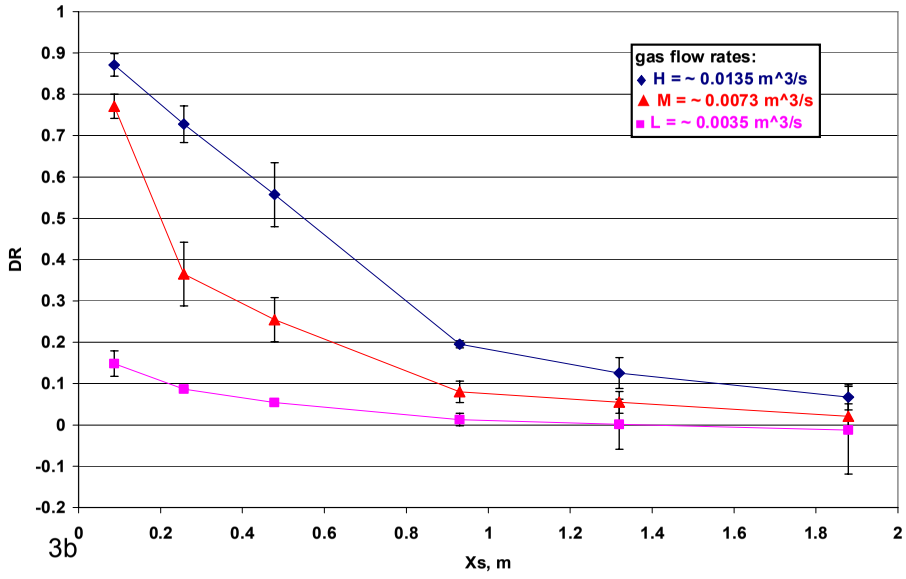

Figure 3. Comparison of drag reduction by polymer and microbubble injection at 16 m/s. 4A) PEO WSR 309 – 500, 1000, 2000 wppm at 5 & 10 Qs. 4b) Microbubble injection.

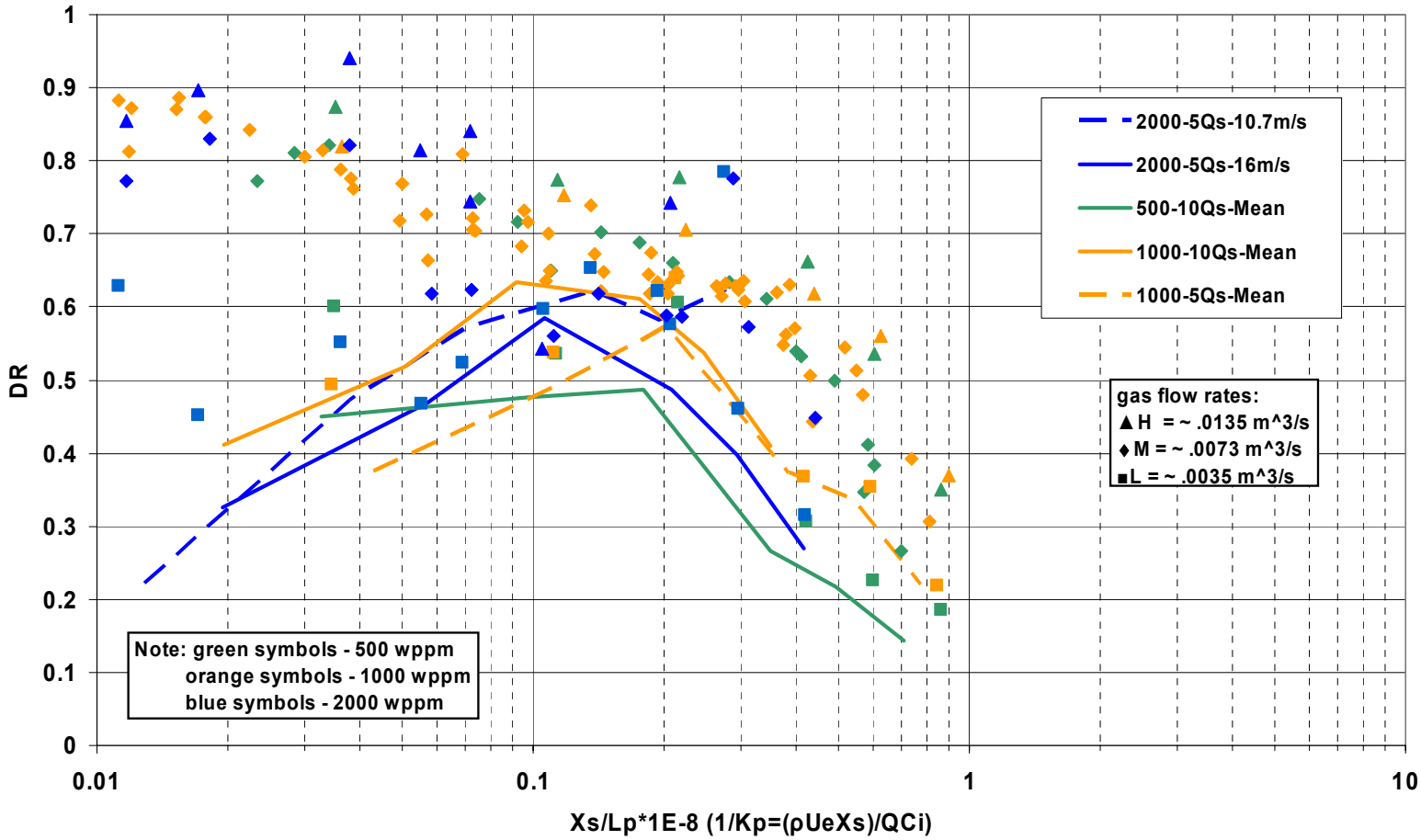

Figure 4. Drag reduction versus Xs/Lp for PEO WSR 309 injection and combined injection.

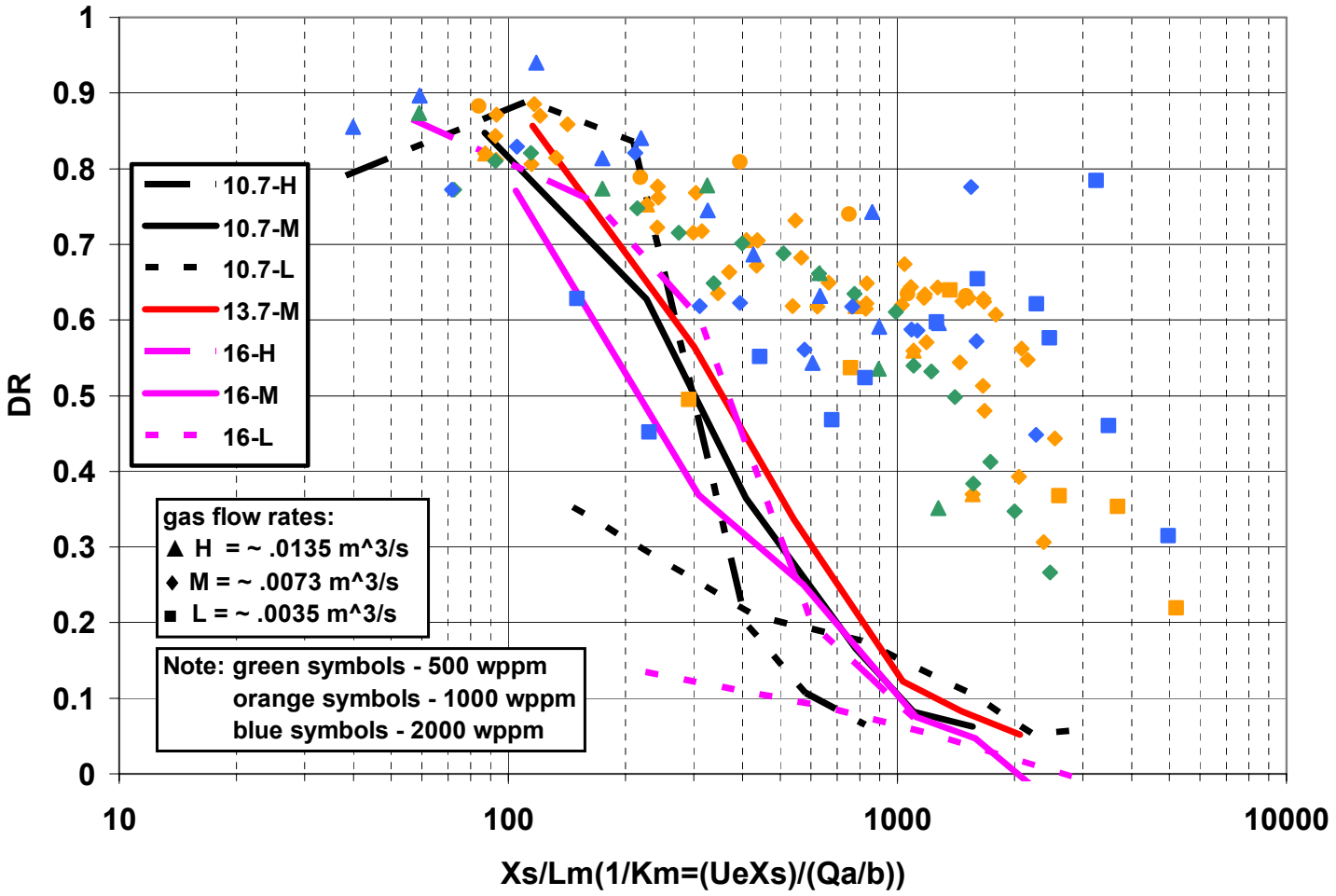

Figure 5. Drag reduction versus Xs/Lm for gas injection and combined injection.

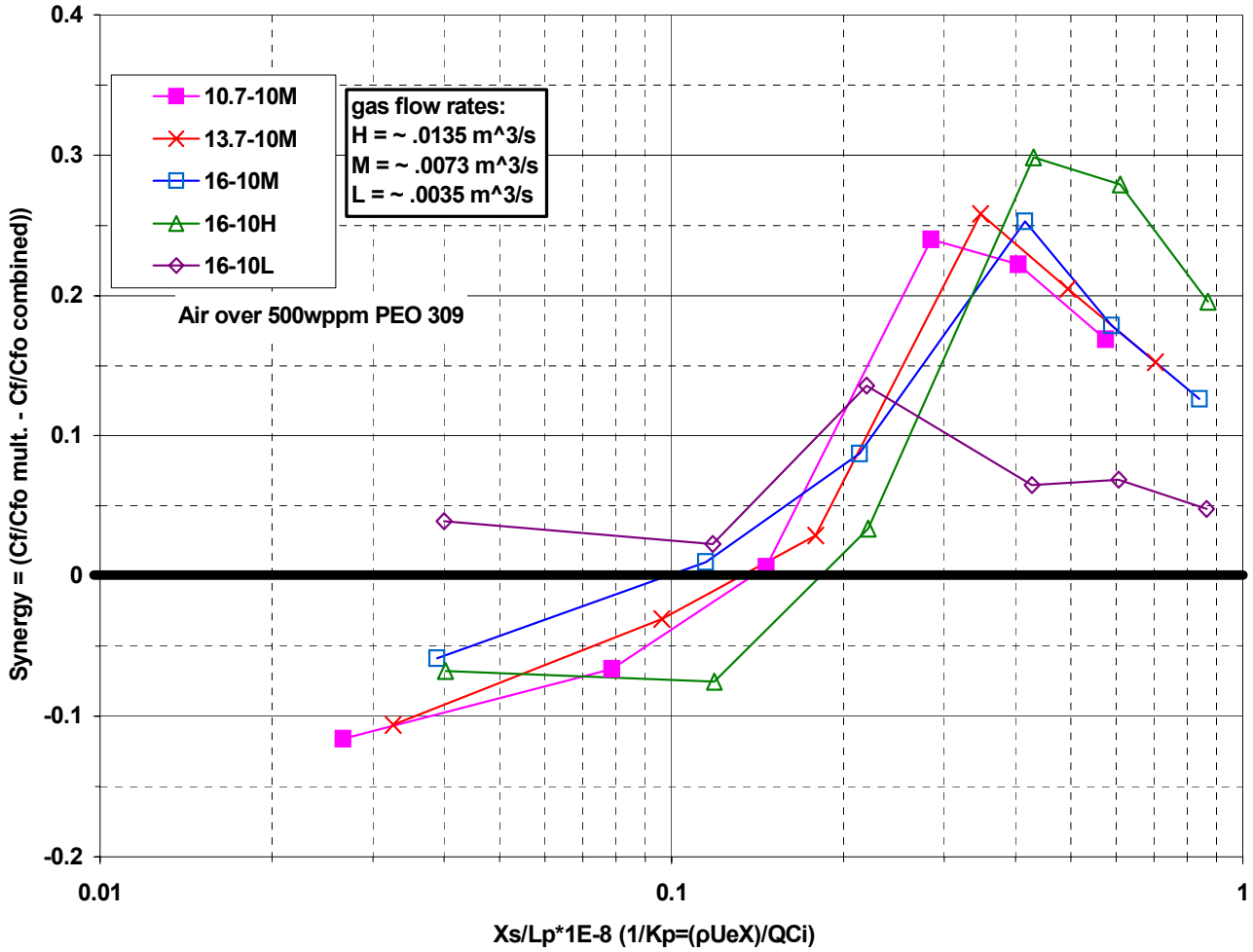

Figure 6. Synergy levels for air over 500 wppm PEO WSR 309.

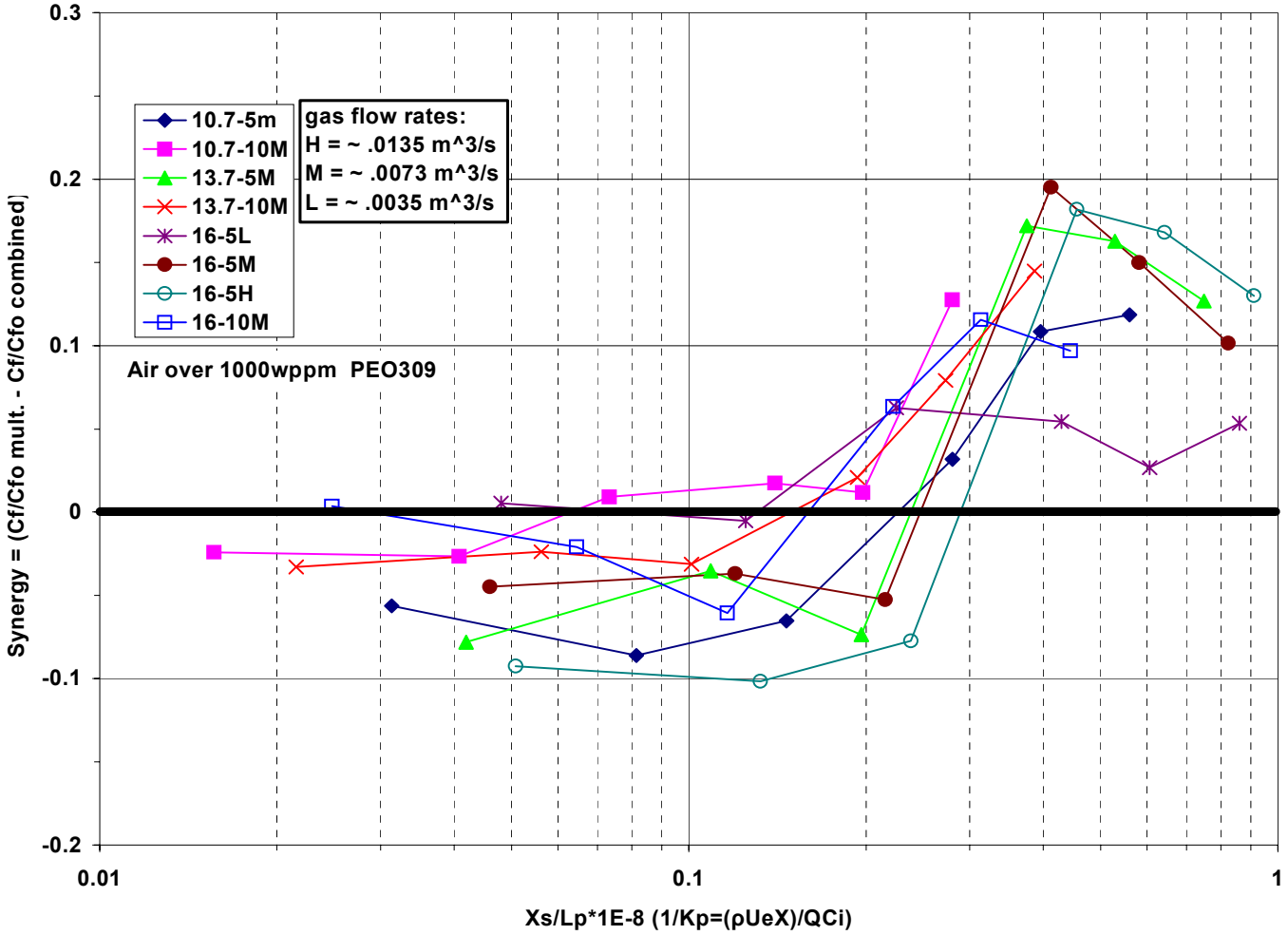

Figure 7. Synergy levels for air over 1000 wppm PEO WSR 309.

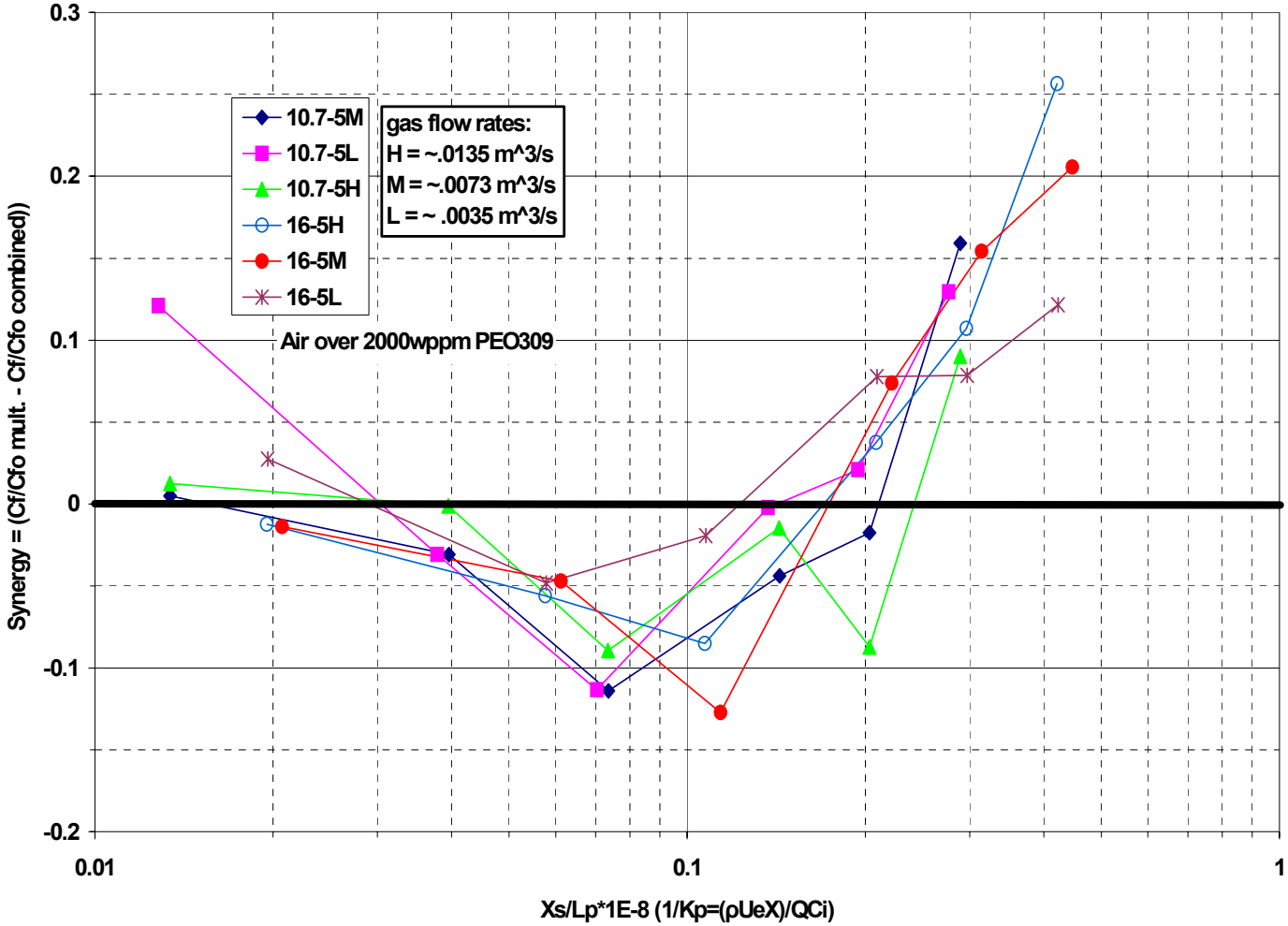

Figure 8. Synergy levels for air over 2000 wppm PEO WSR 309.